

## Synchronization of a laser system to a modulation signal artificially constructed from its strange attractor

Takayuki Tsukamoto,<sup>1</sup> Maki Tachikawa,<sup>2</sup> Takehisa Tohei,<sup>3</sup> Takuya Hirano,<sup>1</sup> Takahiro Kuga,<sup>1</sup> and Tadao Shimizu<sup>4</sup>

<sup>1</sup>*Institute of Physics, University of Tokyo, 3-8-1 Komaba, Meguro-ku, Tokyo 153, Japan*

<sup>2</sup>*Department of Physics, Meiji University, 1-1-1 Higashi-Mita, Tama-ku, Kawasaki 214, Japan*

<sup>3</sup>*Department of Applied Physics, Science University of Tokyo, 1-3 Kagurazaka, Shinjuku-ku, Tokyo 162, Japan*

<sup>4</sup>*Department of Electronics and Computer Science, Science University of Tokyo in Yamaguchi, Onoda 756, Japan*

(Received 20 June 1997; revised manuscript received 14 August 1997)

We demonstrate experimentally and numerically that a laser system can be synchronized to any chaotic pulsation intrinsic to the system by modulating a system parameter. A sequence of pulses is prepared, the heights and interpulse intervals of which are artificially constructed from the correlation function of a prerecorded chaotic pulsation. When an on-off modulation signal obtained from this pulse sequence is applied to intracavity absorption, the laser reproduces the chaotic time sequence. [S1063-651X(97)03012-2]

PACS number(s): 05.45.+b, 42.65.Sf, 42.55.Lt

### I. INTRODUCTION

A great deal of attention has been paid in recent years to developing algorithms to lock a chaotic system to particular pulsations intrinsic to the system. The practical importance of controlling chaos is significant in many fields such as encoded communications [1] and processing in a neural network [2]. The techniques of controlling chaos can be put into two categories: feedback and nonfeedback methods. Feedback techniques are very efficient, and their mechanism is easy to understand. The method first proposed by Ott, Grebogi, and Yorke [3] utilized the property of the strange attractor obtained from a chaotic system, and locked the system to one of its unstable periodic orbits. Since *a priori* knowledge of the system is not necessary, it was widely applied to real physical systems [4]. There are modified versions of this feedback method which were successfully applied to experiments, such as the occasional proportional feedback method [5] and a method using delay coordinates [6]. Nonfeedback methods have the advantage of their speed because they do not require the on-line monitoring and processing. However, their mechanism is less understood. One of the nonfeedback methods is to apply a periodic modulation to a system parameter [7]. This method was applied to laser systems such as a gas laser [8] and a diode laser [9].

With the methods mentioned above, a chaotic system is locked to a periodic pulsation embedded in its strange attractor. On the other hand, Pyragas proposed a method to lock a chaotic system both to a periodic and aperiodic pulsation included in the prerecorded time sequence of a chaotic pulsation [10]. This approach can be considered an application of the synchronization between two unidirectionally coupled chaotic systems [11–13]. In the case of synchronization, the slave system can be locked to the pulsation of the master system. However, it is difficult to realize a particular pulsation intentionally, because the master system has a sensitive dependence on initial conditions and external noises. Pyragas demonstrated that a chaotic system can be synchronized to a chaotic signal which the system itself has already produced [10]. Once the time evolution of the system is recorded, the

present chaotic system can be locked to the aperiodic or periodic pulsation included in the prerecorded history without sensitive dependence on initial conditions or external noises. Pyragas [10] and Peterman, Ye, and Wigen [14] applied this feedback method to an electric circuit and an yttrium iron garnet film in ferromagnetic resonance, respectively. On the other hand, we showed in our previous paper that synchronization to the prerecorded history was done with a nonfeedback method in a CO<sub>2</sub> laser system [15]. In any case, obtainable aperiodic signals are limited to what we have observed in the prerecorded history. To realize a rich variety of pulsation patterns, we have to record the chaotic outputs over a very long period of time.

In this paper, we propose a method to lock a chaotic system to any one of periodic or aperiodic pulsation intrinsic to the system. Our method consists of the following procedures. First, we record the chaotic output from the CO<sub>2</sub> laser. Second, the correlation functions for pulse heights and interpulse intervals characterizing this low-dimensional laser system are obtained from return maps of the prerecorded chaotic pulsation. Now we can choose a time sequence of pulse heights and interpulse intervals (target signal) by successive iteration on the correlation functions. Finally, the modulation signal obtained from this sequence is applied to the intracavity absorption for synchronization of the laser system to the target signal. It is shown both experimentally and numerically that this simple nonfeedback method is quite successful in locking the laser system to an arbitrarily chosen chaotic signal.

### II. EXPERIMENT

The experimental setup of the laser system is shown in Fig. 1. In brief, the CO<sub>2</sub> laser consists of a 2.5-m-long discharge gain tube and a 32-cm-long intracavity absorption cell. The total cavity length is 3.6 m. A gas mixture of CO<sub>2</sub>, N<sub>2</sub>, and He (1:1:8) flows through the laser tube at a total pressure of 8.0 Torr. The laser oscillates on a single mode of TEM<sub>00</sub> at the 9- $\mu$ m P(34) line.

The intracavity cell contains gaseous saturable absorber (CH<sub>3</sub>OH) and buffer gas (SF<sub>6</sub>) of 40 and 115 mTorr, re-

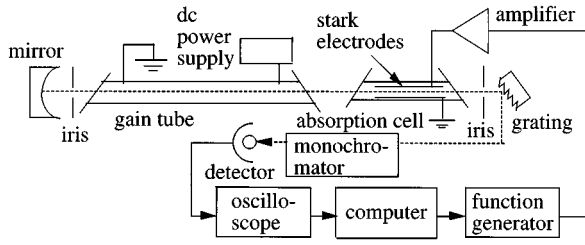


FIG. 1. Experimental setup.

spectively. The absorption cross section of the saturable absorber is modulated by applying dc and ac voltages to the Stark electrodes in the cell. The electrodes consist of two aluminum-coated glass plates which are placed parallel to each other. Each electrode has a dimension of 9.5 cm in length and 3.5 cm in width. The gap between the electrodes is 1.0 cm.

Figure 2 shows the way how to tailor an on-off modulation signal from a sequence of pulses artificially constructed based on the strange attractor of this system. First, we observe a chaotic time sequence and store the sequence in the computer with a sampling rate of 5 MHz. The discharge current is 13.7 mA and dc bias voltage  $V_{\text{bias}}$  applied to the Stark electrodes is 140 V. A part of the time sequence of the recorded pulsation is shown in Fig. 2(a). Here we set a clipping level which is shown with a dotted line in the figure. The interpulse interval  $\Delta t_n$  is defined by the difference  $t_{n+1} - t_n$ , where  $t_n$  is the  $n$ th crossing time at which the laser intensity becomes larger than the clipping level. The correlation between  $\Delta t_n$  and  $X_n$  is shown in Fig. 2(b), where  $X_n$  is the  $n$ th pulse height. The correlation between successive pulse heights  $X_{n+1}$  and  $X_n$  is shown in Fig. 2(c). Data points in Figs. 2(b) and 2(c) are obtained from the whole recorded

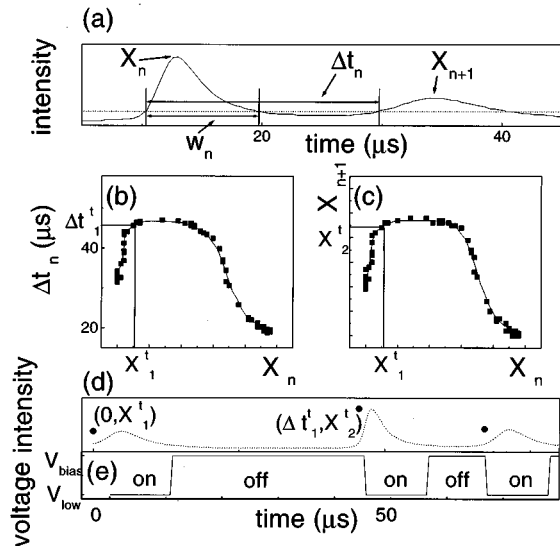


FIG. 2. (a) Time sequence of the prerecorded chaotic pulsation observed at a discharge current of 13.7 mA (the solid line). The dotted line indicates the clipping level. (b) Correlation between  $\Delta t_n$  and  $X_n$ . (c) Correlation between  $X_{n+1}$  and  $X_n$ . (d) A sequence of pulse heights constructed from correlations (the solid circles), and the corresponding time sequence (the dotted line). (e) Modulation signal.

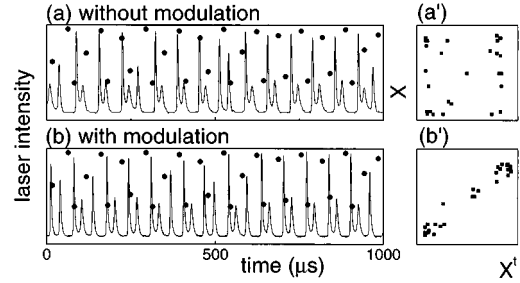


FIG. 3. Experimental results. (a) and (b) Sequence of pulse heights constructed from correlations (the solid circles), and laser output observed at the discharge current of 13.5 mA (the solid curve). (a') and (b') Correlation plots between the corresponding pulse heights.

chaotic pulsation. A one-dimensional correlation is clearly observed in each figure as indicated by a solid curve which is obtained by taking a moving average around each data point and linking those averages. When the initial pulse height is  $X_1^t$ ,  $\Delta t_1^t$ , and  $X_2^t$  are obtained as shown in Figs. 2(b) and 2(c). Thus a sequence of pulse heights and interpulse intervals is artificially constructed as shown by solid circles in Fig. 2(d). In Fig. 2(d), chaotic pulsation that produces these constructed pulse heights and interpulse intervals is depicted by a dotted curve. An on-off modulation signal is obtained from this sequence as shown in Fig. 2(e). The Stark voltage is reduced to  $V_{\text{low}}$  at the moment  $t = \sum_{i=1}^n \Delta t_i^t$  ( $n=0,1,2,\dots$ ), resulting in a decrease of intracavity absorption, and it is restored to the bias voltage at the moment  $t = \sum_{i=1}^n \Delta t_i^t + W$  ( $n=0,1,2,\dots$ ), where  $W$  is the pulse width of the modulation signal. Even though there is a correlation between  $w_n$  and  $X_n$ , where  $w_n$  is the  $n$ th pulse width during when the laser intensity is larger than the clipping level, the pulse width of the modulation signal is fixed at 11  $\mu\text{s}$  for simplicity. We have confirmed that this does not appreciably affect the degree of synchronization. The modulation signal is stored in the wave generator after its high-frequency component is filtered out in order to prevent the amplifier from self-oscillation.

Figures 3(a) and 3(b) show a sequence of pulse heights (the solid circles) constructed from correlations and an observed laser output (the solid curve). The discharge current is set to 13.5 mA, slightly smaller than the previous value. A similar relation between the discharge currents was used to observe the synchronization of the chaotic laser to its prerecorded history [15]. Figures 3(a') and 3(b') show the correlation plots between the pulse heights of the constructed sequence  $X^t$  and the heights of the output pulse  $X$  which appears just after  $t = \sum_{i=1}^n \Delta t_i^t$ . Without modulation, the laser exhibits chaotic pulsation uncorrelated with the target signal as shown in Figs. 3(a) and 3(a'). When the modulation depth is large enough ( $V_{\text{low}}=40$  V), the laser is synchronized to the target signal [Fig. 3(b)]. Data points are located around the straight line,  $X = X^t$ , showing the occurrence of synchronization [Fig. 3(b')]. The laser intensity of the modulated system becomes larger than the clipping level roughly 13  $\mu\text{s}$  after the Stark voltage is reduced.

### III. CALCULATION AND DISCUSSION

We carry out a rate-equation analysis to reproduce the observed dynamics of the modulated  $\text{CO}_2$  laser system. Ac-

TABLE I. Parameters used in the numerical analysis.

$B_{a0}/[B_g f_g(J)]$	$B_g M f_g(J) l_g/L$	$R_1$	$R_2$
900	3820 MHz	300 Hz	380 kHz
$B_{a0} N^* l_a/L$	$k$	$r$	
1.5 MHz	2.0 MHz	6.0 MHz	

cording to the three-level–two-level model which was successfully employed to analyze the passive  $Q$ -switching dynamics in our previous publications [13,15,16], the laser system is described by the following rate equations for the photon density in the lasing mode,  $I$ , the population densities in the upper and lower laser levels,  $M_1$  and  $M_2$ , and the difference in the population density between the upper and lower rotational-vibrational states of the saturable absorber,  $N$ :

$$\begin{aligned}\dot{I} &= B_g f_g(J) I (M_1 - M_2) l_g / L - B_a I N l_a / L - k I, \\ \dot{M}_1 &= -B_g f_g(J) I (M_1 - M_2) + P M - R_1 M_1, \\ \dot{M}_2 &= B_g f_g(J) I (M_1 - M_2) - R_2 M_2, \\ \dot{N} &= -2 B_a I N - r (N - N^*),\end{aligned}$$

where  $B_g$  and  $B_a$  are the cross sections multiplied by the light velocity  $c$  for the induced emission in the gain medium and the absorption in the absorbing medium, respectively. The lengths of the gain tube, the absorption cell, and the laser cavity are denoted as  $l_g$ ,  $l_a$ , and  $L$ , respectively. The fraction of  $\text{CO}_2$  molecules in the rotational level with the quantum number  $J$  is represented by  $f_g(J)$ , the cavity loss rate by  $k$ , and the pumping rate by  $P$ . The vibrational relaxation rates from the upper and lower laser levels to the ground state in the laser medium are written as  $R_1$  and  $R_2$ , respectively.  $r$  is the collisional relaxation rate of the absorbing gas. The total population density of  $\text{CO}_2$  molecules is denoted by  $M$ , and the thermal equilibrium value of  $N$  by  $N^*$ . A detailed formulation of the rate equations is described in Ref. [16]. In this paper, the cross section of the saturable absorber is modulated as

$$B_a = \begin{cases} B_{a0}(1-m) & \text{when the Stark voltage is } V_{\text{low}} \\ B_{a0} & \text{when the Stark voltage is } V_{\text{bias}}, \end{cases}$$

where  $B_{a0}$  and  $m$  are the value of the cross section at the bias voltage and the modulation depth, respectively.

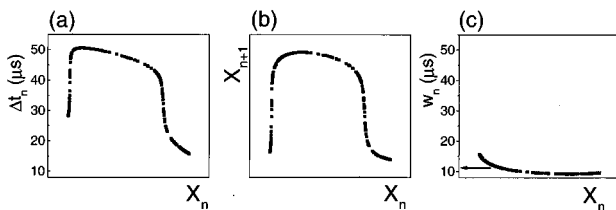


FIG. 4. Correlations obtained from the calculated chaotic pulsation. (a) Correlation between  $\Delta t_n$  and  $X_n$ . (b) Correlation between  $X_{n+1}$  and  $X_n$ . (c) Correlation between  $w_n$  and  $X_n$ . The arrow in (c) shows the value of the pulse width  $W$  used in our calculation.

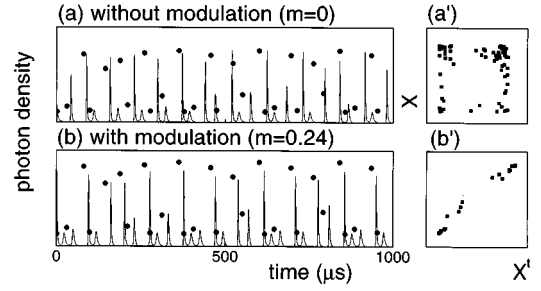


FIG. 5. Calculated results. (a) and (b) Sequence of pulse heights constructed from correlations (the solid circles), and laser output calculated at the pumping rate of 16.45 Hz (the solid curve). (a') and (b') Correlation plots between the corresponding pulse heights.

The observations are successfully reproduced with the parameter values listed in Table I. These values are reasonable for our  $\text{CO}_2$  laser system [15]. The pumping rate of the modulated laser is set to 16.45 Hz, which is slightly smaller than the rate used in calculating the target signal (16.70 Hz). This is consistent with our experiment where the synchronization is observed at the lower discharge current than the prerecorded chaotic pulsation.

Figure 4 shows a correlation between  $\Delta t_n$  and  $X_n$  [Fig. 4(a)], a correlation between  $X_{n+1}$  and  $X_n$  [Fig. 4(b)], and a correlation between  $w_n$  and  $X_n$  [Fig. 4(c)] obtained from the calculated chaotic pulsation. A one-dimensional correlation is clearly observed in each figure. A target sequence of pulse heights and interpulse intervals can be constructed following the procedures described above. Since the variance in  $w_n$  is relatively small, we fix  $w_n$  to a value indicated by an arrow in Fig. 4(c).

Figure 5 shows numerically calculated time series of the target signal and the calculated laser output [Figs. 5(a) and 5(b)], and their pulse heights correlation [Figs. 5(a') and 5(b')]. At a modulation depth of 0.24, which is a value corresponding to the present experimental condition, the laser well reproduces the target signal as shown in Figs. 5(b) and 5(b'). At a larger modulation depth, better synchronization is achieved as shown below. The photon density of the modulated system gets larger than the clipping level  $13 \mu\text{s}$  on average after the intracavity absorption is decreased, which agrees well with the experimental result. The effect of low-pass filtering of the modulation signal is discussed later.

The absorption cross section  $B_a$  is a function of the Stark voltage  $\epsilon$  and is calculated to be

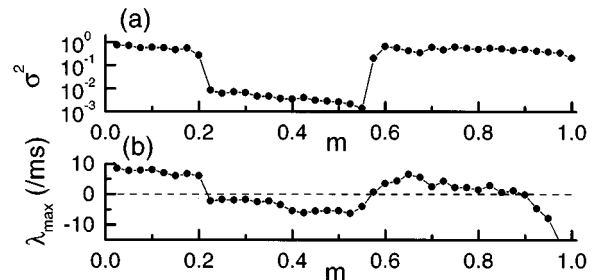


FIG. 6. Numerically obtained variance and largest conditional Lyapunov exponent as a function of the modulation depth.  $N=100$ .

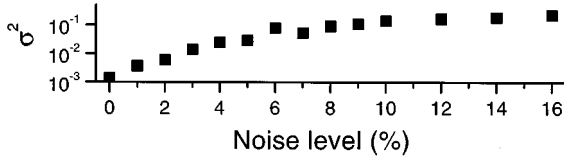


FIG. 7. Numerically obtained minimum variance as a function of the noise level.  $N=100$ .

$$B_a(\epsilon) = B_a(0) \sum_{M, \Delta M} A_{M, \Delta M} \exp\left(-\frac{(\nu_0 + \Delta\nu(\epsilon) - \nu_L)^2}{\Delta\nu_D^2}\right),$$

where  $A_{M, \Delta M}$  is proportional to the transition probability between the  $M$  and  $M + \Delta M$  sublevels.  $\Delta\nu_D$ ,  $\nu_L$ , and  $\nu_0$  are the Doppler width, the laser frequency, and the center frequency of the absorption line, respectively.  $\Delta\nu(\epsilon)$  represents the Stark shift of the relevant energy levels. From this equation the relative decrease in the absorption at the Stark voltage of 40 V is estimated to be 0.2, and this agrees with the value used in the calculation.

The phenomenon of the synchronization is investigated in more detail by numerical analysis. We showed in our previous paper [15] that (1) the variance of the correlation plots from the best-fitted linear relation  $\sigma^2$  is a good index of the synchronization, and that (2) the clipping level should be in such a region that all pulses in the prerecorded history can be distinguished when the history is clipped at this level. The variance  $\sigma^2$  is given as  $\sigma^2 = \sum_{i=1}^N (X_i - aX_i^t)^2 / \sum_i X_i^2$ , where  $X_i^t$ ,  $X_i$ ,  $a$ , and  $N$  are the  $i$ th pulse height of the target signal, the corresponding pulse height of the laser output, the coefficient of the best-fitted linear relation, and the number of data points, respectively. In this paper the clipping level is fixed at a value which gives the smallest variance.

Figure 6 shows the variance and the largest conditional Lyapunov exponent of a calculated time series as a function of the modulation depth. Synchronization is observed in a limited range of the modulation depth,  $0.22 < m < 0.55$ . In this range, the conditional Lyapunov exponent is negative, indicating that the modulated laser system stably follows the target signal. It is interesting to note that there is a range ( $m > 0.9$ ) where the conditional Lyapunov exponent is negative but the variance takes a large value. In this range, detailed analysis shows the synchronization fails intermittently resulting in an increase of the variance. During such time, the modulated laser exhibits pulsation pattern with a quasi-cw tail [17] which is different from the target signal. However, the time sequence does not depend on either initial

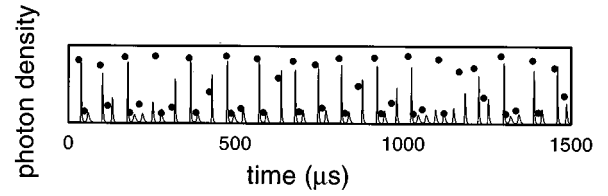


FIG. 8. Sequence of pulse heights constructed from correlations (the solid circles), and calculated laser output when the noise level is 7% (the solid curve).

conditions or external noises, and so the conditional Lyapunov exponent is negative. The similar feature is known as a general synchronization [18].

Further calculations are carried out to consider the effect of the white noise added to the modulation signal. In the modulation signal, intervals between the on states are randomly modified by the noise. The noise level is defined as the ratio of the noise amplitude to the maximum variation of the intervals. For each value of the noise level the variance  $\sigma^2$  is a function of the modulation amplitude, whose minimum value is plotted in Fig. 7. This figure shows that the synchronization occurs at the noise level smaller than 2% (the variance goes below  $10^{-2}$ ). When the noise level exceeds 4%, the laser occasionally becomes unlocked to the target signal, as shown in Fig. 8.

#### IV. CONCLUSION

In conclusion, we have experimentally demonstrated a method by which a chaotic  $\text{CO}_2$  laser system can be locked to any aperiodic pulsation artificially constructed from its strange attractor. The rate-equation analysis has been successfully used to reproduce the observed features of the synchronization.

The advantage of the present method lies in the fact that our choice of the target signal is in principle unlimited if it is intrinsic to the system. For example, the laser can be made to operate on unstable periodic pulsation with period  $n$  obtained from  $n$ th return maps. It may also be applicable to other low-dimensional chaotic systems.

#### ACKNOWLEDGMENTS

One of the authors (T. Tsukamoto) would like to thank JSPS for the partial financial support. This work was partially supported by a Grant-in-Aid from the Ministry of Education, Science, and Culture, Japan.

- [1] K. M. Cuomo and A. V. Oppenheim, Phys. Rev. Lett. **71**, 65 (1993); L. Kocarev and U. Parlitz, *ibid.* **76**, 1816 (1996).
- [2] M. Kushibe *et al.*, Phys. Rev. E **53**, 4502 (1996).
- [3] E. Ott, C. Grebogi, and J. A. Yorke, Phys. Rev. Lett. **64**, 1196 (1990).
- [4] W. L. Ditto, S. N. Rauseo, and M. L. Spano, Phys. Rev. Lett. **65**, 3211 (1990).
- [5] E. R. Hunt, Phys. Rev. Lett. **67**, 1953 (1991); R. Roy, T. W.

Murphy, Jr., T. D. Maier, Z. Gills, and E. R. Hunt, *ibid.* **68**, 1259 (1992).

- [6] K. Pyragas, Phys. Lett. A **170**, 421 (1992); S. Bielawski, D. Drezoiar, and P. Glorieux, Phys. Rev. E **49**, R971 (1994).
- [7] R. Lima and M. Pettini, Phys. Rev. A **41**, 726 (1990).
- [8] R. Meucci, W. Gadomski, M. Ciofini, and F. T. Arecchi, Phys. Rev. E **49**, R2528 (1994); T. Tsukamoto, M. Tachikawa, T. Sugawara, and T. Shimizu, Phys. Rev. A **52**, 1561 (1995).

- [9] N. Watanabe and K. Karaki, *Opt. Lett.* **20**, 1032 (1995).
- [10] K. Pyragas, *Phys. Lett. A* **181**, 203 (1993); A. Kittel, K. Pyragas, and R. Richter, *Phys. Rev. E* **50**, 262 (1994).
- [11] L. M. Pecora and T. L. Carroll, *Phys. Rev. Lett.* **64**, 821 (1990); *Phys. Rev. A* **44**, 2374 (1991).
- [12] R. Roy and K. S. Thornburg, Jr., *Phys. Rev. Lett.* **72**, 2009 (1994).
- [13] T. Sugawara, M. Tachikawa, T. Tsukamoto, and T. Shimizu, *Phys. Rev. Lett.* **72**, 3502 (1994).
- [14] D. W. Peterman, M. Ye, and P. E. Wigen, *Phys. Rev. Lett.* **74**, 1740 (1995).
- [15] T. Tsukamoto, M. Tachikawa, T. Hirano, T. Kuga, and T. Shimizu, *Phys. Rev. E* **54**, 4476 (1996).
- [16] M. Tachikawa, F.-L. Hong, K. Tanii, and T. Shimizu, *Phys. Rev. Lett.* **60**, 2266 (1988).
- [17] M. Tachikawa, K. Tanii, M. Kajita, and T. Shimizu, *Appl. Phys. B* **39**, 83 (1986).
- [18] U. Parlitz, *Phys. Rev. Lett.* **76**, 1232 (1996).